Propylsulfonic Acid-Functionalized Mesoporous Silica Synthesized by in Situ Oxidation of Thiol Groups under Template-Free Condition

Xueguang Wang,[†,‡] Soofin Cheng,*[,†] and Jerry C. C. Chan[†]

Department of Chemistry, National Taiwan University, No. 1, Roosevelt Road, Section 4, Taipei 106, Taiwan, and Research Center for Compact Chemical Process, National Institute for Advanced Industrial Science and Technology (AIST), 4-2-1, Nigatake, Miyagino-ku Sendai, 983-8551 Japan

Received: October 23, 2006; In Final Form: December 8, 2006

Propylsulfonic acid-functionalized mesoporous silica was prepared through in situ oxidization of mercaptopropyl groups with H_2O_2 during a template-free condensation of tetraethyl orthosilicate (TEOS) and 3-mercaptopropyltrimethoxysilane (MPTMS) under strong acidic condition. The obtained materials with 3−15 mol % loadings of sulfonic acid groups had surface areas up to 700 m^2/g and pore sizes around 3.5 nm. The materials synthesized with TEOS prehydrolysis had larger surface areas, pore volumes, and average pore diameters than those synthesized without TEOS prehydrolysis. IR, TG, solid-state NMR, and S K-edge XANES analyses showed that all the mercaptopropyl groups were completely converted to propylsulfonic acid groups without decomposition of the organic moieties using H_2O_2 as the in situ oxidant in the synthesis procedure. The accessibilities of sulfonic acid centers were determined by ion-exchange with cations of various sizes. The functionalized materials were used as acid catalysts in esterification of acetic acid with methanol and acetalization of chlorobenzaldehyde with methanol. The results showed that the propylsulfonic acid-functionalized mesoporous silica prepared with TEOS prehydrolysis and in situ oxidation had similar catalytic activities as propylsulfonic acid-functionalized SBA-15 but higher than the counterparts synthesized without TEOS prehydrolysis or by postoxidation of mercaptopropyl groups with H_2O_2.

1. Introduction

Strong mineral acids, such as H_2SO_4, HF, and $ClSO_3H$ are often used in the synthesis of fine chemicals. The drawbacks of using these liquid acids include corrosion hazard of the reactors, consumption of large amounts of acids, the formation of toxic wastes, and difficulties in product separation and recovery.[1] Thus, great efforts have been made in developing solid acid catalysts to replace liquid acids in the chemical industry.[2,3] Acidic zeolites which have high surface area and confined domains have been widely used in the petrochemical industry.[4−7] However, their uses in liquid-phase organic reactions were often restricted by the small pore diameters of less than 1 nm.

The discovery of mesoporous molecular sieves of the M41S family[8,9] offered large pore sizes in the range of 2−10 nm for the reactions of bulky substrate molecules. However, aluminated mesoporous silica materials like Al-MCM-41 displayed weak acidity in comparison to microporous zeolites.[10] As an alternative, the covalent surface functionalization of mesoporous silica materials with alkylsulfonic acid groups has been reported and successfully used in several acid-catalyzed reactions.[11−25] These hybrid organic−inorganic materials were generally prepared via a postgrafting technique or cocondensation. The cocondensation method is often preferred to the postsynthesis pathway because it minimizes processing steps and provides a more uniform distribution of the organic functionalities.[26] In the literature, propylsulfonic acid-functionalized mesoporous materials were synthesized using 3-mercaptopropyltrimethoxysilane (MPTMS) as the precursor, followed by thiol oxidation with H_2O_2, acidification, and finally washing and drying.[17] Nevertheless, the mesostructure ordering, surface area, pore size, and volume were found to decrease significantly through the postoxidation process.[17,18] In addition, incomplete oxidation of thiol groups or formation of disulfide S−S species were often observed on the resultant materials.[25,27] Margolese et al.[28] improved the cocondensation method by introducing hydrogen peroxide into the synthesis mixture and in situ oxidation of thiol groups. The obtained mesoporous materials had uniform pore sizes, high surface areas, and high thermal stabilities after removal of the surfactant by refluxing with ethanol. The sulfonic acid-functionalized mesoporous materials prepared by such an in situ oxidation route are very promising for replacement of liquid acid catalysts. However, the uses of expensive pore-directing agents and large amounts of organic solvents to remove the templates make these catalysts impracticable from the commercial point of view. Besides, these organic functionalized ordered materials did not have good mechanical strength. After chemical reactions, the ordering of the mesopores often decreased or completely collapsed. These problems could be avoided using amorphous silica with organic functionalities with rigid cross-linking skeletons by preparing the organic functionalized silica through direct hydrolysis of the precursors without using the template agents.[27,29−31]

In the present paper, we report the preparation of propylsulfonic acid-functionalized mesoporous silica through a simple cocondensation of TEOS and MPTMS without the addition of any pore-directing agent. The thiol groups of MPTMS were in situ oxidized to sulfonic acid groups with H_2O_2 under acidic

*Corresponding author. Phone: +886-2-23638017. Fax: +886-2-23636359. E-mail: chem1031@ntu.edu.tw.
† National Taiwan University.
‡ National Institute for Advanced Industrial Science and Technology.

10.1021/jp066924b CCC: $37.00
Published on Web 01/18/2007

condition. The obtained materials were characterized by N_2 adsorption−desorption measurement, FTIR, TG, solid-state NMR, S K-edge XANES, and elemental analysis (EA). The accessibility of the sulfonic acids in the materials was determined by ion-exchange capacities with aqueous solutions of sodium chloride (NaCl), tetramethylammonium chloride (TMAC), and tetrabutylammonium chloride (TBAC). Esterification of acetic acid with methanol and acetalization of chlorobenzaldehyde with methanol were used to test the catalytic activities of the materials. The obtained materials were compared with sulfonic acid-functionalized SBA-15 materials in the accessibility of the acid sites and the catalytic activity.

2. Experimental Section

2.1. Chemicals and Synthesis. 3-Mercaptopropyltrimethoxysilane and block copolymer Pluronic P123 ($EO_{20}PO_{70}EO_{20}$, M_{av} = 5800) were purchased from Aldrich. Other chemicals of reagent grade were from Acros. All chemicals were used as received.

The sulfonic acid-functionalized mesoporous silica materials were prepared by one-pot cocondensation of tetraethoxysilane (TEOS) and MPTMS in the presence of H_2O_2 under acidic condition. In the typical procedure, 8 g of TEOS was first added into an opening beaker with 125 mL of 2.0 M HCl aqueous solution and hydrolyzed at 40 °C under stirring for 20 h. At this time the mixture became a slightly viscous solution; the appropriate amount of MPTMS and aqueous solution of H_2O_2 (35 wt %) were slowly added in the solution, and the mixture was kept stirring at the same temperature until the water was dried out, and finally the solid was dried at 100 °C overnight and ground to powder. The MPTMS/H_2O_2 molar ratio was 1/10, and the MPTMS/(TEOS + MPTMS) ratio was varied from 0 to 0.15, or 0−15%. The resultant samples are referred as SiO_2−SO_3H-*x*-P, where P means "prehydrolysis of TEOS" and *x* is the MPTMS/(TEOS + MPTMS) molar percentage. For example, SiO_2−SO_3H-10-P represents the sample prepared with TEOS prehydrolysis and MPTMS/(TEOS + MPTMS) = 10 mol %. For comparison, samples were also prepared by simultaneous mixing of TEOS and MPTMS or without TEOS prehydrolysis. They are labeled as SiO_2−SO_3H-*x*-S. Another sample containing 10 mol % MPTMS was prepared with TEOS prehydrolysis in the absence of H_2O_2 and is denoted as SiO_2−SH-10-P. The thiol groups in SiO_2−SH-10-P were postoxidized to sulfonic acid groups with a 20-fold excess of aqueous solution of H_2O_2 (35 wt %) at room temperature for 24 h, and then the solids were acidified with aqueous solution of 10 wt % H_2SO_4, followed by filtration, washing with water and ethanol, and finally drying at 100 °C. The postoxidized sample was defined as SiO_2−SO_3H-10-Po.

Propylsulfonic acid-functionalized SBA-15 materials were prepared according to the literature.[28] An amount of 4 g of Pluronic 123 was dissolved in 125 g of 2.0 M HCl aqueous solution at room temperature. After adding TEOS, the resultant solution was equilibrated at 40 °C for 45 min, and then MPTMS was slowly added into the solution. The molar composition of the mixture was (1 − *y*)TEOS/*y*MPTMS/9*y*H_2O_2/5.8HCl/0.017P123/165H_2O, where the *y* value varied from 5% to 15%. The resulting mixtures were stirred at 40 °C for 20 h and then transferred into a polypropylene bottle and reacted at 90 °C under static condition for 24 h. The solid products were recovered by filtration and dried at room temperature overnight. The template was removed by refluxing with ethanol. Finally, the materials were filtered, washed several times with water and ethanol, and dried at 50 °C. Similarly, the samples were denoted as SBA-SO_3H-5, -10, and -15, respectively.

2.2. Sample Characterization. N_2 adsorption−desorption isotherms were measured using a Micromeritics Tristar 3000 at liquid nitrogen temperature. Before the measurements, the samples were degassed at 120 °C overnight. The specific surface areas were evaluated using the Brunauer−Emmett−Teller (BET) method in the p/p_0 range of 0.05−0.3. Pore size distribution curves were calculated using the desorption branch of the isotherms and the Barrett−Joyner−Halenda (BJH) method, and pore sizes (Dp) were obtained from the peak positions of the distribution curves, and average pore diameter (Da) values were calculated by BJH method. The pore volume was taken at the p/p_0 = 0.990 point.

X-ray powder diffraction (XRD) patterns were obtained on a PANalytical X'Pert Pro diffractometer using Cu Kα radiation (λ = 1.5418 Å) at 45 kV and 40 mA.

Thermogravimetric (TG) analyses were carried out on a Netzsch TG 951 thermogravimetric analyzer with a heating speed of 10 °C/min in an air flow of 50 mL/min. Fourier transform infrared (FTIR) spectra were taken on a Nicolet Magna-IR 550 spectrometer with a resolution of 2 cm^{-1} using the KBr method.

Sulfur K-edge X-ray adsorption near-edge structure (XANES) spectroscopy was performed at beam line 15B at the Synchrotron Radiation Research Center Facility situated on the 1.5 GeV electron storage ring at Hsinchu, Taiwan. The operating beam current was 200 mA, and the photon energies were calibrated using the L-edge of pure Mo foil.

Sulfur elemental analyses (EA) were performed on a Heraeus CHNS elemental analyzer. The accessibility of sulfonic acid centers in the materials was determined by ion-exchange with cations of various sizes followed by acid titration.[12,28] Aqueous solutions of sodium chloride (NaCl, 2 M), tetramethylammonium chloride (TMAC, 0.05 M), and tetrabutylammonium chloride (TBAC, 0.05 M) were used as the exchange agents. In a typical experiment, 0.10 g of solid treated at 200 °C for 1 day was added to 20 mL of aqueous solution containing the corresponding salt. The resultant suspension was equilibrated for 6 h, then filtered and washed with a small amount of water, and finally the filtrate was titrated potentiometrically by dropwise addition of aqueous solution of 0.01 M NaOH.

The NMR experiments were carried out at ^{29}Si, ^{13}C, and ^{1}H frequencies of 59.6, 75.5, and 300.1 MHz, respectively, on a Bruker DSX300 NMR spectrometer equipped with a commercial 7 mm MAS NMR probe. All spectra were measured at room temperature. The magic-angle spinning frequencies were set to 5 kHz for all experiments, and the variation was limited to ±3 Hz using a commercial pneumatic control unit. Chemical shifts were externally referred to tetramethylsilane for ^{29}Si and ^{13}C. For the ^{29}Si Bloch-decay experiment, the recycle delay was set to 60 s. $^{13}C\{^{1}H\}$ cross-polarization spectra were measured with a recycle delay of 4 s, and the contact times were 1.5 ms. During the contact time the ^{1}H nutation frequency was set equal to 50 kHz, and a linear ramping was applied to the nutation frequencies of ^{13}C (27.3−43.0 kHz). The proton decoupling field during the acquisition period was 83 kHz.

2.3. Catalytic Reactions. Before the reaction, the catalysts were treated at 200 °C for 1 day to remove adsorbed water in the materials. The esterification of acetic acid with methanol was carried out in a two-necked flask of 50 mL with a reflux condenser which was placed in a thermostatic bath with a magnetic stirrer. In a typical experiment, 0.15 mol (9.08 g) of acetic acid and 0.15 mol (4.81 g) of methanol were mixed under vigorous stirring and heated to 50 °C of the reaction temperature and then 0.15 g of the treated catalyst was added into the

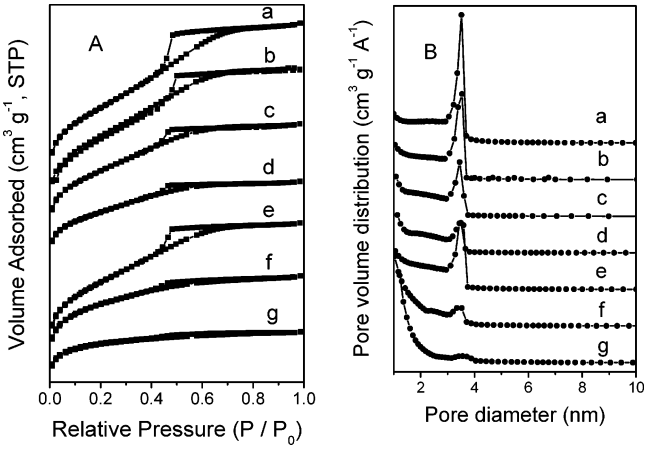

Figure 1. Nitrogen adsorption−desorption isotherms (A) and BJH pore size distribution (B) of the sulfonic acid-functionalized silica materials. (a) SiO_2-SO_3H-3-P, (b) SiO_2-SO_3H-7-P, (c) SiO_2-SO_3H-10-P, (d) SiO_2-SO_3H-15-P, (e) SiO_2-SO_3H-7-S, (f) SiO_2-SO_3H-10-S, and (g) SiO_2-SO_3H-15-S.

reaction mixture. Initial reaction rates were determined during the first 10 min of the reaction (the conversion of the reaction was <10 mol %). Quantitative analysis was based on the calculated response factors for the appropriate reactants and the corresponding reaction products. The overall mass balance was more than 98%.

Acetalization of chlorobenzaldehyde with methanol was performed in a one-necked flask of 50 mL. An amount of 10 mmol (1.41 g) of chlorobenzaldehyde was dissolved into 25 mL of methanol under vigorous stirring and kept at 30 °C, then 20 mg of the catalyst was added into the reaction mixture. An amount of 0.4 g of anisole was used as the internal standard. Initial reaction rates (mol g^{-1} s^{-1}) were determined during the first 5 min of the reaction, where the conversion of the reaction was less than 25 mol %. The overall balance based on the reactant was more than 95%. In all cases, the liquid products were separated from the reaction mixture at appropriate reaction intervals with a filtering syringe and analyzed using a Chrompak CP 9000 gas chromatograph (GC) equipped with a 30 m × 0.53 mm RTX-50 capillary column and FID detector and identified by gas chromatography−mass spectrometry (HP5971 GC−MS with a 30 m × 0.25 mm RTX-50 capillary column).

3. Results and Discussion

3.1. Characterization of Sulfonic Acid-Functionalized Amorphous Silica. The N_2 adsorption−desorption isotherms of the sulfonic acid-functionalized materials are illustrated in Figure 1A. The samples prepared with prehydrolysis of TEOS exhibit characteristic type IV isotherms with apparent hysteresis loops, which are typical of mesoporous materials according to the IUPAC classification. The amount of adsorbed N_2 decreases with MPTMS content in the initial gel (Figure 1A, curves a−d). In comparison to the results of samples prepared with TEOS prehydrolysis, those prepared without TEOS prehydrolysis have type IV isotherms only when the MPTMS contents in the initial gel were lower than 7%. As the MPTMS increases up to 15 mol %, the isotherm is closer to the type I characteristic and no apparent hysteresis is observed (Figure 1A, curve g). BJH pore size analysis in Figure 1B, curves a−d, shows that the materials with prehydrolysis of TEOS contain mesopores of narrow pore size distributions (~1.0 nm PSD, estimated from the peak width at half-maximum height) centered around 3.5 nm, and the mesopores volume reduces as the amount of MPTMS increases

TABLE 1: Physical and Textural Properties of Functionalized Amorphous Silica and SBA-15 Materials with MPTMS

sample	Dp (nm)[a]	Da (nm)[b]	S_{BET} (m^2/g)	micropore S.A. (m^2/g)[c]	pore volume (cm^3/g)
SiO_2	3.6	3.3	754	1	0.62
SiO_2-SO_3H-3-P	3.5	3.2	678	0	0.54
SiO_2-SO_3H-7-P	3.5	2.9	690	0	0.50
SiO_2-SO_3H-10-P	3.5	2.6	612	0	0.40
SiO_2-SO_3H-15-P	3.5	2.5	486	74	0.31
SiO_2-SO_3H-7-S	3.4	2.8	679	0	0.47
SiO_2-SO_3H-10-S	3.4	2.4	571	0	0.34
SiO_2-SO_3H-15-S		2.2	421	228	0.23
SiO_2-SH-10-P	3.6	3.5	721	0	0.63
SiO_2-SO_3H-Po	3.6	3.1	723	0	0.56
$SBA-SO_3H$-5	6.5	5.3	872	51	1.16
$SBA-SO_3H$-10	6.2	5.3	867	25	1.14
$SBA-SO_3H$-15	3.6	3.1	706	135	0.54

[a] The peak positions of the distribution curves by BJH. [b] Average pore diameter by BET. [c] Calculated by *t*-plot curves.

in the synthesis mixture. Relatively, only the sample containing 7 mol % MPTMS without TEOS prehydrolysis shows a narrow pore distribution at 3.4 nm (Figure 1B, curve e). The samples with higher MPTMS contents contain very low mesopores volumes. These results illustrate that mesoporous structures with narrow PSD can be formed by cocondensation of TEOS and an appropriate amount of MPTMS in strong acid environment without the addition of pore-directing agents. However, TEOS prehydrolysis is necessary in order to form mesostructural functionalized materials of narrow PSD.

Powder X-ray diffraction analyses were performed on all the MPTMS-functionalized materials. The samples without pore-directing agent showed no reflection peaks, indicating no long-range ordering of the mesopores in these materials by the template-free route. This is in contrast to functionalized SBA-15 samples, which have one intense peak and two weak peaks, indexed to (100), (110), and (200) diffractions, respectively, characteristic of materials with ordered hexagonal arrays of one-dimensional channel structure.[32]

The basic physicochemical and textural properties of the functionalized materials are shown in Table 1. All the samples prepared by cocondensation of TEOS and MPTMS show high surface areas and the BJH pore sizes (Dp) around 3.5 nm. The surface area and the pore volume decrease as the MPTMS content is increased from 3 to 15 mol % in the synthesis mixture. Although the BJH pore sizes are similar, the average pore size (Da) reduces with the increase in the MPTMS content, indicating the increase in the amount of small pores in the materials. Comparatively, the samples prepared without TEOS prehydrolysis show lower surface areas, smaller pore volumes, and smaller average pore sizes than their counterparts synthesized with TEOS prehydrolysis. Microporous surfaces of the functionalized materials calculated by *t*-plot curves are also shown in Table 1. It is noticeable that the samples containing 15 mol % MPTMS in the initial mixture have relatively large microporous surface areas, similar to those of SBA-15 materials, in which there always exist certain micropores in the mesostructural walls. Moreover, the ones prepared without TEOS prehydrolysis have extremely high microporous surface areas. In contrast, the samples containing MPTMS of less than 10 mol % in the initial mixture show no microporous surface areas.

Thermogravimetric analyses were conducted to determine the amount of organic functional groups incorporated in the materials, and the TGA and DTG profiles are shown in Figure 2. For the sample synthesized without H_2O_2, SiO_2-SH-10-P

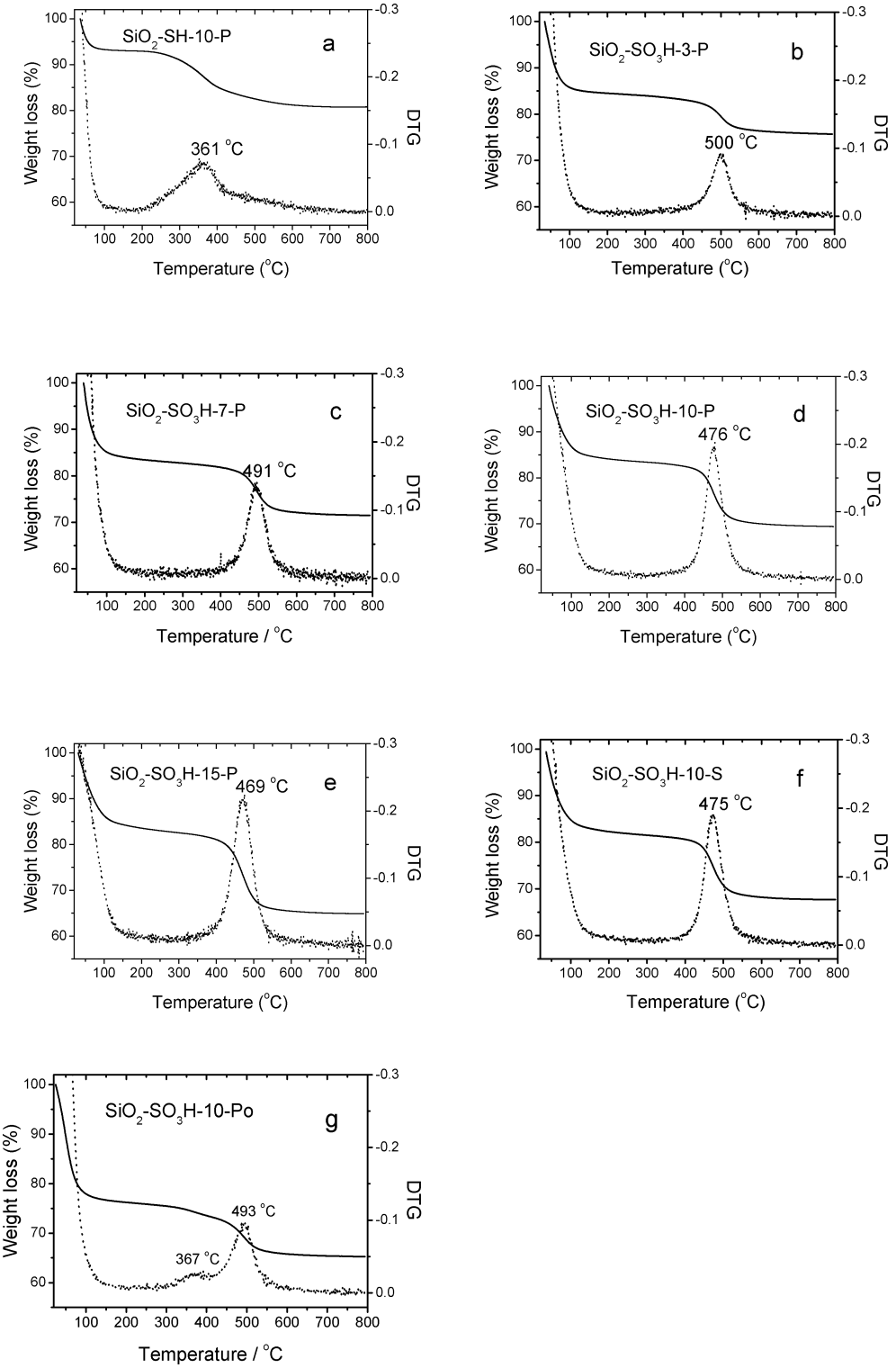

Figure 2. TGA and DTG profiles of functionalized silica with different MPTMS contents in the initial mixture in the presence or absence of H_2O_2.

has a small weight loss lower than 100 °C due to the desorption of water and a weight loss at 200−400 °C due to the decomposition of mercaptopropyl groups (Figure 2a). All the samples synthesized in the presence of H_2O_2 have a weight loss greater than 15% at temperatures lower than 100 °C, indicating the hydrophilic nature of these samples and the conversion of thiol to sulfonic acid groups by H_2O_2 during the synthesis. Another weight loss in the range of 400−600 °C is attributed to the decomposition of propylsulfonic acid groups incorporated in the materials, which increases from 7 to 18 wt % as the MPTMS content is increased from 3 to 15 mol % (Figure 2, parts b−f). Moreover, the decomposition temperature decreases from 500 to 469 °C as the amount of MPTMS increases, indicating that the stability of organic moieties in the materials decreases. This is probably due to the incomplete condensation of the methoxy groups of MPTMS onto the framework as the intermolecular interaction between the organic moieties on the surface of the materials increases.

In comparison of the functionalized samples synthesized with and without TEOS hydrolysis, SiO_2-SO_3H-10-P and SiO_2-SO_3H-10-S have almost the same decomposition temperature of organic moieties as shown in Figure 2, parts d and f,

TABLE 2: Sulfur Contents and Acid Capacities of Functionalized Amorphous Silica and SBA-15 Materials with MPTMS

	S content (mmol/g)			acid capacity (mmol/g)		
sample	theor	by EA	by TG	NaCl	TMAC	TBAC
SiO_2-SO_3H-3-P	0.50	0.64	0.66	0.55	0.50	0.49
SiO_2-SO_3H-7-P	1.03	1.02	1.00	0.95	0.82	0.68
SiO_2-SO_3H-10-P	1.40	1.40	1.35	1.40	1.04	0.74
SiO_2-SO_3H-15-P	1.94	1.91	1.80	1.73	1.24	0.80
SiO_2-SO_3H-7-S	1.03	1.02	1.04	0.98	0.81	0.64
SiO_2-SO_3H-10-S	1.40	1.42	1.37	1.30	0.99	0.66
SiO_2-SO_3H-15-S	1.94	1.85	1.79	1.81	1.02	0.58
SiO_2-SH-10-P	1.40	1.40	1.33	0.08	0.08	0.12
SiO_2-SO_3H-10-Po	1.40	1.39	1.35	0.84	0.76	0.65
$SBA-SO_3H$-5	0.76	0.59	0.63	0.57	0.56	0.58
$SBA-SO_3H$-10	1.40	1.05	1.13	1.04	0.96	0.83
$SBA-SO_3H$-15	1.94	1.40	1.50	1.36	1.11	0.81

illustrating that the preparation method has no influence on the thermal stability of the materials. For the sample synthesized with TEOS prehydrolysis but posttreated with H_2O_2, SiO_2-SO_3H-10-Po shows a large weight loss of water at temperatures lower than 100 °C and a broad weight loss at higher temperatures (Figure 2g). The DTG resolves the latter peak to two weight losses. The intense peak centered around 490 °C should correspond to the decomposition of propylsulfonic acid groups, and the small shoulder centered around 370 °C corresponds to the thiol groups. These results indicate that thiol groups were not oxidized completely to sulfonic acid groups in the posttreatment procedure with H_2O_2, as also described in the literatures.[25,27]

Sulfur elemental contents in the MPTMS-functionalized materials were analyzed by TG and EA, and the results are given in Table 2. It can be seen that MPTMS in the initial mixture was mostly incorporated into the silica materials through the template-free routes. For the samples of very low MPTMS loading, the S contents are greater than the theoretical values, probably due to the empirical deviation in weighing and transferring the small amounts of MPTMS. Comparatively, only 70 to ~80 mol % of MPTMS was incorporated in propylsulfonic acid-functionalized SBA-15 materials.

Qualitative identification of the organic functional groups in the materials has also been performed by FTIR spectra. Figure 3 illustrates the FTIR spectra of the functionalized materials with 10 mol % MPTMS prepared by different routes and that of reference pure silica prepared by TEOS hydrolysis. The typical Si−O−Si bands around 1220, 1070, 791, and 470 cm^{-1} associated with the condensed silica network are present in all cases. For the reference silica, no absorbance peaks in the low-frequency range of 1300−1500 cm^{-1} and high-frequency range of 2750−3000 cm^{-1}, corresponding to the C−H vibration, reveals that the ethoxy groups in TEOS are completely hydrolyzed in the synthesis condition.[33] After addition of MPTMS, the weak absorbances at 1470 and 1420 cm^{-1} were assigned to bending vibrations of methylene groups, and a broad absorbance in the range of 2850−3000 cm^{-1} corresponding to the methylene stretching vibrations of the propyl chains appears, indicating the incorporation of the organic moiety. For the samples prepared without H_2O_2, a weak peak appeared at 2580 cm^{-1} and was assigned to the S−H stretching (Figure 3, curve e), which was not seen for the samples prepared in the presence of H_2O_2 (Figure 3, curves b and c), demonstrating that the thiol groups have been oxidized. These results are in agreement with the TG experiments. For the postoxidized sample SiO_2-SO_3H-10-Po (Figure 3, curve d), although TG analysis showed the incomplete oxidation of the thiol group, the peak associated with

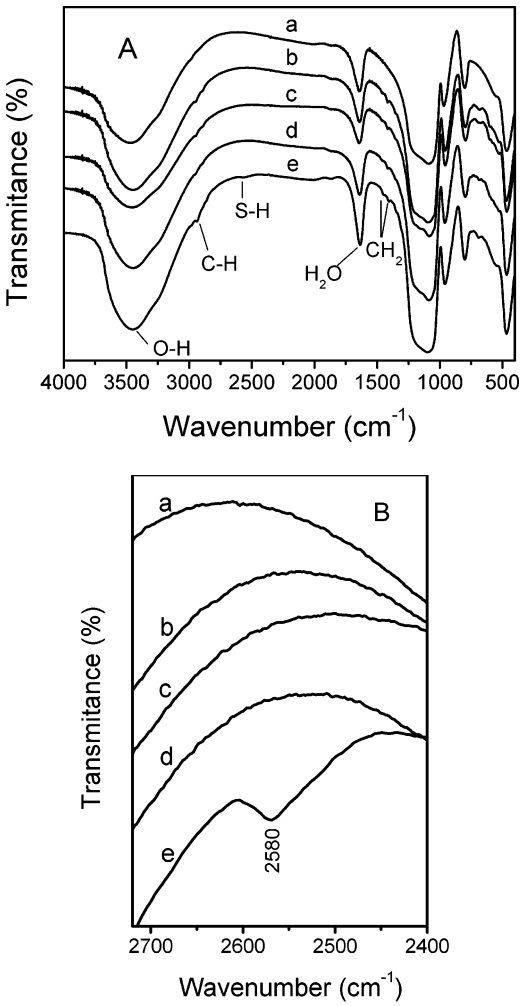

Figure 3. FTIR spectra of (a) pure SiO_2 reference, (b) SiO_2-SO_3H-10-P, (c) SiO_2-SO_3H-10-S, (d) SiO_2-SO_3H-10-Po, and (e) SiO_2-SH-10-P (the whole range in (A) and amplification between 2400 and 2720 cm^{-1} in (B)).

the S−H bond is also not seen in its IR spectrum. That is likely due to the low absorption coefficient of the S−H stretching.[34] The peaks corresponding to the S═O stretching vibrations of sulfonic acid are normally observed in the range of 1000−1200 cm^{-1}. However, these peaks cannot be resolved due to their overlap with the absorbance of the Si−O−Si stretch in the 1000−1130 cm^{-1} range and that of the Si−CH_2−R stretch in the 1200−1250 cm^{-1} range. For all the samples, the peaks associated with the noncondensed Si−OH groups at 960 cm^{-1} are present, and the strong peak around 1630 cm^{-1} is mainly from the bending vibration of adsorbed H_2O.

Solid-state ^{13}C and ^{29}Si NMR spectroscopies proved to be the most useful for providing chemical information regarding the condensation of organosiloxane and siloxane. ^{29}Si MAS NMR spectra of functionalized silica materials containing 10 mol % MPTMS in the mixture in the presence of H_2O_2 are shown in Figure 4. Three distinct resonances for siloxane [Q^n = $Si(OSi)_n(OH)_{4-n}$, $n = 2-4$; Q^2 at −92; Q^3 at −101; Q^4 at −110 ppm] and two other resonances for organosiloxane [T^m = $RSi(OSi)_m(OH)_{3-m}$, $m = 1-3$; T^2 at −57; T^3 at −67 ppm] are clearly observed. The appearance of T^m peaks with T^3 predominant over T^2 confirms that the organosiloxane precursors are effectively condensed as a part of the silica framework.[35] The relative integrated intensities of the T^m and Q^n signals ($T^m/(T^m + Q^n)$) are both ca. 0.11 for SiO_2-SO_3H-10-P and SiO_2-SO_3H-10-S, in good agreement with those theoretically expected

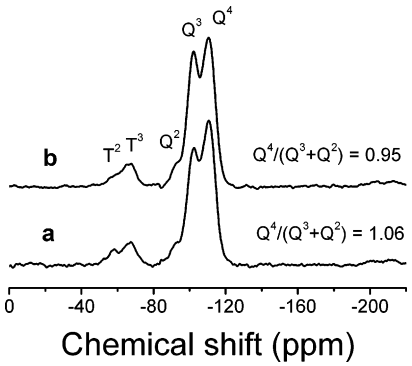

Figure 4. ^{29}Si MAS NMR spectra of functionalized silica materials containing 10 mol % MPTMS in the initial mixture (a) with and (b) without TEOS prehydrolysis.

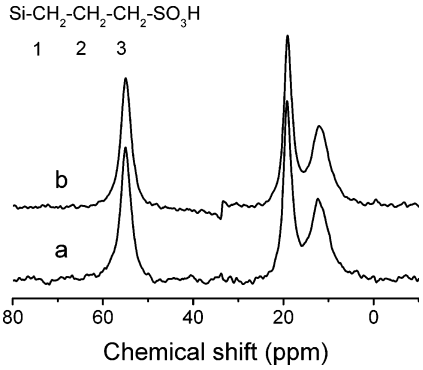

Figure 5. ^{13}C CP MAS NMR spectra of functionalized silica materials containing 10 mol % MPTMS in the initial mixture (a) with and (b) without TEOS prehydrolysis.

on the basis of the composition of MPTMS in the initial mixture. Moreover, the relative area ratio of $Q^4/(Q^3 + Q^2)$ for SiO_2-SO_3H-10-P is slightly greater than that of SiO_2-SO_3H-10-S, indicating that more complete TEOS condensation was achieved when it was prehydrolyzed for 20 h before the organosiloxane was added into the synthesis mixture.

The ^{13}C CP MAS NMR spectra of the functionalized silica materials containing 10 mol % MPTMS in the mixture in the presence of H_2O_2 are illustrated in Figure 5. Three distinct peaks at 11.5, 19.2, and 55.1 ppm, corresponding to the C atoms on the $Si-CH_2-CH_2-CH_2-SO_3H$ group, are clearly displayed in sequence from left to right.[28] This further confirms that MPTMS precursors are cocondensed into the prepared sample and the organic moieties are not decomposed during the preparation procedure. There are no additional resonance signals at 29 and 22.4 ppm, which are assigned to the central carbon atom and the carbon atom adjacent to the SH moiety of the propyl chain in the 3-mercaptopropyl moiety,[34] respectively, showing that all the thiol groups are oxidized in the synthesis procedure. In addition, there is no evidence of the presence of other sulfur compounds such as disulfide species ($-CH_2-S-S-CH_2-$, 36.5 ppm) and thiosulfonate species ($-CH_2-S-S(O_2)-CH_2-$, 39 ppm) arising from incomplete oxidation of mercaptopropyl groups.[17,27,34,36] These results indicate that the mercaptopropyl groups were completely converted into propylsulfonic acids. Besides, no resonance NMR shift signals at 60 ppm, assigned to the carbon (adjacent to the O atom) of ethoxy groups ($Si-OCH_2CH_3$), and at 52 ppm, corresponding to the carbon atom of methoxy groups ($Si-OCH_3$), shows that both TEOS and MPTMS precursors are completely hydrolyzed in the preparation procedure.[37] These results are also supported by the IR spectra in Figure 3.

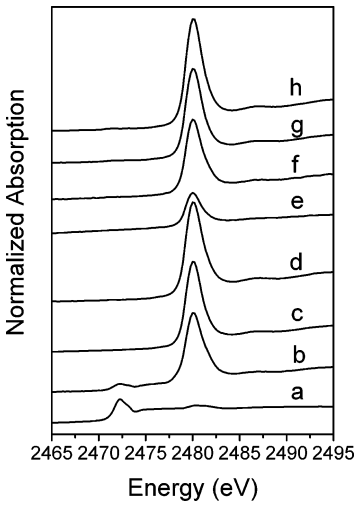

Figure 6. Sulfur K-edge XANES spectra of functionalized amorphous silica: (a) SiO_2-SH-10-P, (b) SiO_2-SO_3H-10-Po, (c) SiO_2-SO_3H-10-S, (d) SiO_2-SO_3H-15-S, (e) SiO_2-SO_3H-3-P, (f) SiO_2-SO_3H-7-P, (g) SiO_2-SO_3H-10-P, and (h) SiO_2-SO_3H-15-P.

X-ray absorption near-edge structure (XANES) spectroscopy is very sensitive to the electronic structure, oxidation state, and local symmetry of the absorbing site compared to classical methods of chemical characterization of sulfur-containing compounds. Sulfur K-edge XANES spectroscopy has been effectively used to study sulfur speciation in various natural systems.[38−40] The increase in absorption energy (E_k) and intensity of the white line (i.e., main adsorption peak) with increasing formal oxidation state allows us to identify and quantify the different sulfur species present in the sample.[39] Figure 6 shows the S K-edge XANES spectra of the sulfonic acid or thiol-functionalized materials prepared through different routes. For SiO_2-SH-10-P prepared in the absence of H_2O_2, the main peak in Figure 6, curve a, is observed at 2472 eV, corresponding to S in the thiol groups. After postoxidation with H_2O_2, a strong absorbance appears at 2480 eV (Figure 6, curve b), which corresponds to S in the sulfonic acid groups of +5 state. In comparison to the S K-edge XANES spectra of SiO_2-SH-10-P and SiO_2-SO_3H-10-Po, the thiol groups are not completely oxidized by postoxidation with H_2O_2 as has been reported in the literature.[27,34] From Figure 6, curves a and b, it is difficult to identify other sulfur species arising from the incomplete oxidation of the S−H groups due to the interference of the oscillations situated after the white line of the thiol groups at 2472 eV. As for the samples prepared in the presence of H_2O_2, the absorbances associated with the S−H groups completely disappear and the white lines shift to higher energy position around 2480 eV, accompanied by no peaks from 2472 to 2480 eV. These results indicate that thiol groups were completely converted into sulfonic acid groups by in situ oxidation, consistent with the TG and ^{29}Si NMR results. The residue of the thiol groups or other sulfur species from incomplete oxidation of thiol groups is negligible.

The accessibility of sulfonic acid centers in the propylsulfonic acid-functionalized materials was taken by determining the acid capacities by acid−base titration using different ion-exchange agents, and the results are shown in Table 2. When sodium chloride was used as the ion-exchange agent, the acid capacities of the materials prepared in the presence of H_2O_2 increased with the MPTMS contents in the initial mixture. The acid capacity values are very close to those from EA or TG analyses, further confirming the complete oxidation of thiol groups. In contrast, the SiO_2-SO_3H-10-Po sample obtained by postoxidation shows

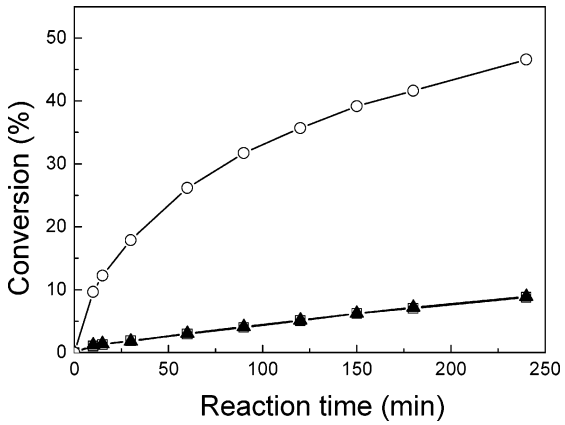

Figure 7. Catalytic esterification of acetic acid with methanol as a function of reaction time at 50 °C over sulfonic acid-functionalized silica (○), in comparison to the results over pure silica (▲) and without solid catalysts (homogeneous reaction) (□).

lower acid capacity value than that from EA or TG analyses, attributed to the incomplete oxidation of the thiol groups.

As the larger size cations such as TMA^+ and TBA^+ were used as the ion-exchange agents, the acid capacities decreased, and the discrepancy between acid capacity and the value from EA increased with the sizes of cations, as illustrated in Table 2. The preparation method has influence on the accessibility of the acid sites in the materials. For the samples containing the same MPTMS contents, the ones prepared with TEOS prehydrolysis always have higher acid capacities than those without prehydrolysis. According to N_2 adsorption, the materials obtained with TEOS prehydrolysis contain higher pore volume and less microporous surface area than those without TEOS prehydrolysis and they have mesopores mainly in the range of 3 to ~4 nm in diameter, which are much larger than the cation diameters. In contrast, the sample synthesized without TEOS prehydrolysis, especially SiO_2-SO_3H-15-S, has high micropore surface area, which is likely not accessible by the large cations. It is also noticeable that the acid capacities of the samples prepared with TEOS prehydrolysis have similar acid capacities as the propylsulfonic acid-functionalized SBA-15 based on samples with the same MPTMS contents in the initial mixtures.

3.2. Catalytic Reactions. Esterification of acetic acid with methanol and acetalization of chlorobenzaldehyde with methanol were used to test the catalytic activities of propylsulfonic acid-functionalized materials in liquid-phase reactions. The activities in the reactions were expressed by methanol conversion for esterification and by chlorobenzadehyde conversion for acetalization, respectively. No byproducts other than methyl acetate and 1-chloro-4-dimethoxymethyl-benzene for esterification and for acetalization, respectively, were observed by GC−MS or GC.

The catalytic performance of the SiO_2-SO_3H-10-P catalyst in esterification at 50 °C as a function of reaction period is illustrated in Figure 7. The methanol conversion increases dramatically and almost linearly with reaction time in the first 15 min. Then, the reaction rate slows down as the reaction time prolongs. After 4 h, a conversion around 47% was obtained. Figure 7 also shows that esterification could proceed in the absence of the solid acid catalysts. However, the methanol conversions in homogeneous system without solid catalysts or over pure silica were very low. Even after 4 h, the conversions were less than 9%.

Table 3 shows the initial rates and turnover frequencies (TOFs) of esterification and acetalization over different catalysts. The initial rates (mol g^{-1} s^{-1}) for esterification over the solid acid catalysts were defined as those subtracted by the initial homogeneous rates during the first 10 min of the reactions. The TOFs, expressed in s^{-1}, were calculated by dividing the initial rates in the first 10 min by the acid sites. It can be seen that the initial rates of all the catalysts prepared by different synthetic routes increase with the sulfonic acid loadings and get to the maximum at 10 mol % sulfonic acid loading. The propylsulfonic acid-functionalized materials prepared with TEOS prehydrolysis in the presence of H_2O_2 show higher initial activities than the counterparts prepared without TEOS prehydrolysis or by postoxidation and have close activities to those of propylsulfonic acid-functionalized SBA-15.

The TOFs in esterification of all the catalysts prepared by different synthetic routes based on the acid capacities determined with different cation exchangers were found to increase in the order of $Na^+ < TMA^+ < TBA^+$. Moreover, the TOF values were all around 1.8×10^{-1} s^{-1} when the acid capacities were determined with TBA^+. These results imply that the acid centers which could be exchanged with TBA^+ are the effective catalytic sites for esterification. Similar TOF values were observed for the amorphous silica catalysts prepared without TEOS prehydrolysis except the one with highest MPTMS contents (SiO_2-SO_3H-15-S). A possible explanation is that a portion of the propylsulfonic groups might interact with each other through hydrogen bonding and is not effective in catalytic reactions.

In the case of acetalization of chlorobenzaldehyde with methanol, the catalysts prepared with TEOS prehydrolysis show

TABLE 3: Initial Rates and Turnover Frequencies Based on Acid Capacities for Esterification of Acetic Acid with Methanol and Acetalization of Chlorobenzaldehyde and Methanol over Sulfonic Acid-Functionalized Silica Materials

	initial rate × 10^4 (mol/g s)		TOF[b] × 10 (s^{-1}) based on acid sites determined by					
			NaCl		TMACl		TBACl	
sample	ester[a]	acetal	ester[a]	acetal	ester[a]	acetal	ester[a]	acetal
SiO_2	0	0.3						
SiO_2-SO_3H-3-P	0.9	0.7	1.6	1.3	1.8	1.4	1.8	1.4
SiO_2-SO_3H-7-P	1.2	3.1	1.3	3.3	1.5	3.8	1.8	4.6
SiO_2-SO_3H-10-P	1.4	3.3	1.0	2.4	1.3	3.2	1.9	4.5
SiO_2-SO_3H-15-P	1.3	2.6	0.8	1.5	1.0	2.1	1.6	3.3
SiO_2-SO_3H-7-S	1.2	1.4	1.2	1.4	1.5	1.7	1.9	2.2
SiO_2-SO_3H-10-S	1.2	2.5	0.9	1.9	1.2	2.5	1.8	3.8
SiO_2-SO_3H-15-S	0.7	1.2	0.4	0.7	0.7	1.2	1.2	2.1
SiO_2-SO_3H-10-Po	1.3	2.3	1.5	2.7	1.7	3.0	2.0	3.5
$SBA-SO_3H$-5	1.1	0.7	1.9	1.2	2.0	1.2	1.9	1.2
$SBA-SO_3H$-10	1.4	3.5	1.3	3.4	1.5	3.6	1.7	4.2
$SBA-SO_3H$-15	1.4	3.5	1.0	2.6	1.3	3.2	1.7	4.3

[a] The value subtracted by the initial rate in the homogeneous reaction value. [b] Turnover frequency.

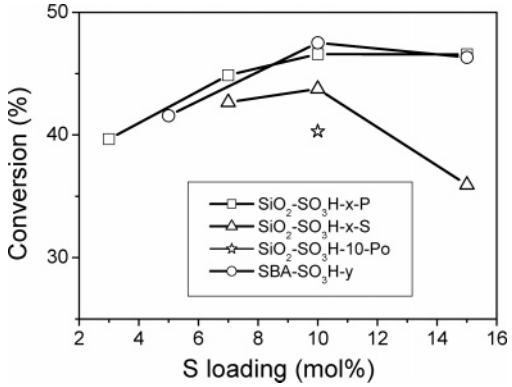

Figure 8. Catalytic activities of sulfonic acid-functionalized silica materials with different MPTMS contents in the initial mixture in esterification of acetic acid with methanol at 50 °C for 4 h.

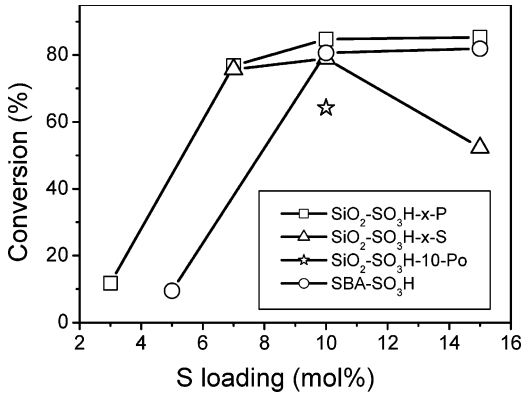

Figure 9. Catalytic activities of sulfonic acid-functionalized silica materials with different MPTMS contents in the initial mixture in acetalization of chlorobenzaldehyde with methanol at 30 °C for 1 h.

higher TOFs than those without TEOS prehydrolysis. However, the TOF values over various catalysts did not approach a constant even when the acid capacities were determined with TBA^+. The extremely low TOFs for the catalysts with low MPTMS contents imply that the acetalization reaction probably needs more than two acid sites to catalyze the reaction.

Figures 8 and 9 display the catalytic activities for the esterification of acetic with methanol after 4 h of reaction at 50 °C and the acetalization of chlorobenzaldehyde with methanol after 1 h at 30 °C, respectively, over the catalysts with different MPTMS contents. It can be seen that the in situ oxidized functionalized catalysts have similar conversions as the functionalized SBA-15 with the same MPTMS contents in the initial mixtures and higher than the catalysts prepared without TEOS prehydrolysis or the catalyst by postoxidation. For the acetalization reaction, very low catalytic activities were observed over the catalysts with low MPTMS contents (SiO_2-SO_3H-3-P and SBA-SO_3H-5), and that is likely due to low acid densities on the surface of these catalysts.

In order to test the stability of the catalyst in the liquid phase, the SiO_2-SO_3H-10-P catalyst used in the esterification and the acetalization reactions were recycled five times after the used catalyst was washed with methanol. The results are shown in Figure 10. For the esterification, the catalytic activities are almost unchanged, demonstrating that the catalyst can be used repeatedly under the present conditions. As for the acetalization, the catalytic activities gradually decrease with the recycling number but still show about 60% conversion after five times, indicating the high stability of the catalyst in this reaction.

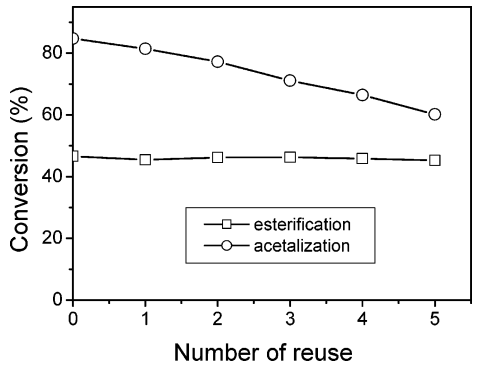

Figure 10. Dependency of catalytic activity on reuse number over SiO_2-SO_3H-10-P for esterification of acetic acid with methanol at 50 °C for 4 h and for acetalization of chlorobenzaldehyde with methanol at 30 °C for 1 h.

4. Conclusions

The functionalized silica materials with different loadings of propylsulfonic acid groups were prepared by a simple cocondensation of TEOS and MPTMS under acidic condition. The resultant materials contained mesoporous structures with narrow pore size distribution. Samples prepared with TEOS prehydrolysis showed larger surface areas and pore volumes than those without TEOS prehydrolysis. Thiol groups could be completely in situ oxidized into sulfonic acid groups in the synthesis procedure when H_2O_2 was also added in the synthesis mixture. The sulfonic acid centers in the materials prepared with TEOS prehydrolysis were more accessible by large reactive molecules compared with those of the counterparts without TEOS prehydrolysis. When used as acid catalysts in liquid-phase reactions, the propylsulfonic acid-functionalized silica with TEOS prehydrolysis have better catalytic activities than the counterparts without TEOS prehydrolysis or by postoxidation with H_2O_2 for esterification of acetic acid with methanol and acetalization of chlorobenzaldehyde with methanol. Moreover, the activities are comparable to that of propylsulfonic acid-functionalized SBA-15 of ordered mesoporous structure. This synthesis method opens up a new synthesis route which avoids the use of expensive templates and large amount of organic solvents for preparation of mesoporous organic−inorganic hybrid catalysts.

Acknowledgment. This project was supported by the National Science Council, Taiwan.

References and Notes

(1) Wilson, K.; Clark, J. H. *Pure Appl. Chem.* **2000**, *72*, 1313.
(2) Okuhara, T. *Chem. Rev.* **2002**, *102*, 3641.
(3) Clark, J. H.; Butterworth, A. J.; Tavener, S. J.; Teasdale, A. J.; Barlow, S. J.; Bastock, T. W.; Martin, K. *J. Chem. Technol. Biotechnol.* **1997**, *68*, 367.
(4) Davis, M. E. *Microporous Mesoporous Mater.* **1998**, *21*, 173.
(5) Sheldon, R. A.; Elings, J. A.; Lee, S. K.; Lempers, H. E. B.; Downing, R. S. *J. Mol. Catal. A: Chem.* **1998**, *134*, 129.
(6) Corma, A.; Garcia, H. *Catal. Today* **1997**, *38*, 257.
(7) Hölderich, W. F.; Hesse, M.; Näumann, F. *Angew. Chem., Int. Ed. Engl.* **1988**, *27*, 226.
(8) Kresge, C. T.; Leonowicz, M. E.; Roth, W. J.; Vartuli, J. C.; Beck, J. S. *Nature* **1992**, *359*, 710.
(9) Beck, J. S.; Vartuli, J. C.; Roth, W. J.; Leonowicz, M. E.; Kresge, C. T.; Schmitt, K. D.; Chu, C. T. W.; Olson, D. H.; Sheppard, E. W.; McCullen, S. B.; Higgins, J. B.; Schlenker, J. L. *J. Am. Chem. Soc.* **1992**, *114*, 10834.
(10) Corma, A.; Fornes, V.; Navarro, M. T.; Perez-Pariente, J. *J. Catal.* **1994**, *148*, 569.
(11) Diaz, I.; Mohino, F.; Perez-Pariente, J.; Sastre, E. *Appl. Catal., A* **2001**, *205*, 19.

(12) Melero, J. A.; Stucky, G. D.; Van Grieken, R.; Morales, G. *J. Mater. Chem.* **2002**, *12*, 1664.
(13) Yang, Q.; Kapoor, M. P.; Inagaki, S. *J. Am. Chem. Soc.* **2002**, *124*, 9694.
(14) Shen, J. G. C.; Herman, R. G.; Klier, K. *J. Phys. Chem. B* **2002**, *106*, 9975.
(15) Wilson, K.; Lee, A. F.; Macquarrie, D. J.; Clark, J. H. *Appl. Catal., A* **2002**, *228*, 127.
(16) Cano-Serrano, E.; Campos-Martin, J. M.; Fierro, J. L. G. *Chem. Commun.* **2003**, 246.
(17) Rhijn, V. M. V.; De Vos, D. E.; Sels, B. F.; Bossaert, W. D.; Jacobs, P. A. *Chem. Commun.* **1998**, 317.
(18) Lim, M. H.; Blanford, C. F.; Stein, A. *Chem. Mater.* **1998**, *10*, 467.
(19) Das, D.; Lee, J. F.; Cheng, S. F. *Chem. Commun.* **2001**, 2178.
(20) Mbaraka, I. K.; Shanks, B. H. *J. Catal.* **2005**, *229*, 365.
(21) Mbaraka, I. K.; Radu, D. R.; Lin, V. S. Y.; Shanks, B. H. *J. Catal.* **2003**, *219*, 329.
(22) Wang, X. G.; Chen, C. C.; Chen, S.; Mou, Y.; Cheng, S. *Appl. Catal., A* **2005**, *281*, 47.
(23) Hamoudi, S.; Kaliaguine, S. *Microporous Mesoporous Mater.* **2003**, *59*, 195.
(24) Mikhailenko, S.; Desplantier-Giscard, D.; Kanumah, C.; Kaliaguine, S. *Microporous Mesoporous Mater.* **2002**, *52*, 29.
(25) Ganesan, V.; Walcarius, A. *Langmuir* **2004**, *20*, 3623.
(26) Walcarius, A.; Delacote, C. *Chem. Mater.* **2003**, *15*, 4181.
(27) Cano-Serrano, E.; Blanco-Brieva, G.; Campos-Martin, J. M.; Fierro, J. L. G. *Langmuir* **2003**, *19*, 7621.
(28) Margolese, D.; Melero, J. A.; Christiansen, S. C.; Chmelka, B. F.; Stucky, G. D. *Chem. Mater.* **2000**, *12*, 2448.
(29) Badley, R. D.; Ford, W. T. *J. Org. Chem.* **1989**, *54*, 5437.
(30) Mdoe, J. E. G.; Clark, J. H.; Macquarrie, D. J. *Synlett* **1998**, 625.
(31) Shimizu, K.; Hayashi, E.; Hatamachi, T.; Kodama, T.; Kitayama, Y. *Tetrahedron Lett.* **2004**, *45*, 5135.
(32) Zhao, D.; Feng, J.; Huo, Q.; Melosh, N.; Frederichson, G. H.; Chmelka, B. F.; Stucky, G. D. *Science* **1998**, *279*, 548.
(33) Sartori, G.; Bigi, F.; Maggi, R.; Sartorio, R.; Macquarrie, D. J.; Lenarda, M.; Storaro, L.; Coluccia, S.; Martra, G. *J. Catal.* **2004**, *222*, 410.
(34) Diaz, I.; Marquez-Alvarez, C.; Mohino, F.; Perez-Pariente, J.; Sastre, E. *J. Catal.* **2000**, *193*, 283.
(35) Sadasivan, S.; Khushalani, D.; Mann, S. *J. Mater. Chem.* **2003**, *13*, 1023.
(36) Van, Rhijn, W. M.; De Vos, D.; Bossaert, W.; Bullen, J.; Wouters, B.; Grobet, P. J.; Jacobs, P. A. *Stud. Surf. Sci. Catal.* **1998**, *117*, 183.
(37) Guo, W.; Park, J. Y.; Oh, M. O.; Jeong, H. W.; Cho, W. J.; Kim, I. K.; Ha, C. S. *Chem. Mater.* **2003**, *15*, 2295.
(38) Huffman, G. P.; Shah, N.; Huggins, F. E.; Stock, L. M., Chatterjee, K.; Kilbane, J. J.; Chou, M.; Buchanan, D. H. *Fuel* **1995**, *74*, 549.
(39) Sarret, G.; Connan, J.; Kasrai, M.; Bancroft, G. M.; Charrie-Duhaut, A. Lemoine, S.; Adam, P.; Albrecht, P.; Eybert-berard, L. *Geochim. Cosmochim. Acta* **1999**, *182*, 156.
(40) Kasrai, M.; Bancroft, G. M.; Brunner, R. W.; Jonasson, R. G.; Brown, J. R.; Tan, K. H.; Feng, X. *Geochim. Cosmochim. Acta* **1994**, *58*, 2865.